Published in final edited form as:
J Am Chem Soc. 2011 March 30; 133(12): 4558–4566. doi:10.1021/ja110715f.

The aggregation-enhancing Huntingtin N-terminus is helical in amyloid fibrils

V.N. Sivanandam[‖,‡,§], **Murali Jayaraman**[‖,‡,†], **Cody L. Hoop**[‡], **Ravindra Kodali**[‡,†], **Ronald Wetzel**[‡,†], and **Patrick C.A. van der Wel**[*,‡]

[‡]Department of Structural Biology, University of Pittsburgh School of Medicine, Biomedical Science Tower 3, 3501 Fifth Ave, Pittsburgh, Pennsylvania 15260, USA

[†]Pittsburgh Institute for Neurodegenerative Diseases, University of Pittsburgh School of Medicine, Biomedical Science Tower 3, 3501 Fifth Ave, Pittsburgh, Pennsylvania 15260, USA

Abstract

The 17-residue N-terminus (htt^{NT}) directly flanking the polyQ sequence in huntingtin (htt) N-terminal fragments plays a crucial role in initiating and accelerating the aggregation process that is associated with Huntington's disease (HD) pathogenesis. Here we report on magic-angle-spinning solid state NMR studies of the amyloid-like aggregates of an htt N-terminal fragment. We find that the polyQ portion of this peptide exists in a rigid, dehydrated amyloid core that is structurally similar to simpler polyQ fibrils and may contain anti-parallel β-sheets. In contrast, the htt^{NT} sequence in the aggregates is composed in part of a well-defined helix, which likely also exists in early oligomeric aggregates. Further NMR experiments demonstrate that the N-terminal helical segment displays increased dynamics and water exposure. Given its specific contribution to the initiation, rate and mechanism of fibril formation, the helical nature of htt^{NT} and its apparent lack of effect on the polyQ fibril core structure seem surprising. The results provide new details about these disease-associated aggregates, and also provide a clear example of an amino acid sequence that greatly enhances the rate of amyloid formation while itself not taking part in amyloid structure. There is an interesting mechanistic analogy to recent reports pointing out the early stage contributions of transient intermolecular helix-helix interactions in the aggregation behavior of various other amyloid fibrils.

Keywords

Amyloid fibrils; solid-state NMR; magic-angle-spinning

Introduction

At least nine human diseases are associated with mutations that extend the length of a polyQ-encoding CAG repeat in a corresponding disease protein[1]. Since neurons in brain tissue from these diseases exhibit polyQ-rich aggregates[2], and since polyQ peptides in vivo[3]

pvdwel@pitt.edu.
[‖]These authors contributed equally.
[§]Present address: Department of Chemistry & Biochemistry, 251 Nieuwland Science Hall, University of Notre Dame du Lac, Notre Dame, Indiana 46556

Supporting Information Available. Table of chemical shift assignments, additional secondary structure analysis schematics, 2D ^{13}C-^{13}C spectrum of L7-A10 interresidue contact, additional ^{13}C 1D spectra, dynamical NMR data on labeled peptides, table of labeled peptides and amounts, additional pulse sequence schematics and experimental details. This material is available free of charge via the Internet at http://pubs.acs.org.

and in vitro[4,5] exhibit repeat length dependent aggregation kinetics, there is considerable interest in the role of protein aggregation in the disease mechanisms. The only common element in these disease proteins, the expanded polyQ sequence, in isolation aggregates by a nucleated growth mechanism without any non-amyloid intermediates[6–8]. While some polyQ flanking sequences do not alter this fundamental mechanism[9–11], in other cases the flanking sequence can play a dramatic role by kinetically overriding the normal polyQ nucleation mechanism[10,12,13]. The nature of the flanking sequences also has direct consequences for the aggregate morphology and observed toxicity[14–16]. In the protein huntingtin (htt), which is responsible for Huntington's disease (HD), a short and moderately hydrophobic 17 amino acid N-terminal sequence (htt^{NT}) flanking the polyQ sequence plays an enormous role in stimulating aggregation and altering the aggregation mechanism[10,17,18]. In N-terminal fragments similar to the likely toxic proteolysis products[19] of the htt protein, the htt^{NT} sequence dramatically enhances aggregation rates in vivo[20] and in vitro[10,17], apparently by mediating the rapid formation of spherical oligomers with the htt^{NT} segment at their core[10]. Interestingly, most other protein sequences that form amyloid also appear to spontaneously assemble in vitro via the intermediate formation of similar oligomeric structures[21–23].

Understanding this mechanism and its products in greater detail may reveal new approaches for intervention in aggregate formation in HD and other disorders. In spite of several experimental[10,17,18] and computational[24,25] studies, much remains to be learned. Central questions include the structural transformations from monomer to oligomer to fibril for each of the separate domain segments, and how these domains might interact to further affect mechanism and rate. Fibrils formed by polyQ peptides without flanking domains are known to consist of β-sheet structure[26,27], analogous to other amyloids. The mechanisms by which flanking sequences can modulate polyQ aggregation mechanisms and/or rates are varied. A polyPro segment C-terminal to polyQ slows aggregation, apparently by altering the distribution of various polyQ conformations in the low molecular weight, soluble ensemble[9,28,29]. In several other cases, the flanking sequence instead aids or initiates polyQ aggregation by virtue of its own propensity for amyloid formation. In the disease protein ataxin-3 (AT-3), the large Josephin domain initiates aggregation by forming an amyloid structure itself, which then directly or indirectly propagates into the polyQ segment[12]. Similarly, in an artificial polyQ protein formed by fusion of polyQ to cellular retinoic acid binding protein (CRABP), CRABP aggregates first, followed by polyQ amyloid formation[30]. In both cases, the Josephin and CRABP domains alone have an independent folded conformation, but are capable of aggregating into amyloid fibrils under appropriate conditions.

As an aggregation-assisting domain, the htt^{NT} segment has some interesting differences to these two cases, both in terms of its innate structure and its ability to form amyloid in isolation. The htt^{NT} sequence by itself exhibits tediously slow aggregation kinetics[10] and, on aggregation, forms oligomeric structures, similar to the intermediates of htt N-terminal fragment aggregation, but fails to progress to amyloid structure. In terms of its structure, simulations[31] and structure-propensity calculations[17] predict htt^{NT} to exist in an α-helical conformation, but a sequence-based analysis of intrinsic structure indicates only a modest tendency toward order[10]. Experimentally, monomeric htt^{NT} exhibits no stable secondary structure by solution NMR[10], but displays a degree of α-helicity in CD spectra[10,16,25]. There is little direct information on the structural transformations undergone by htt^{NT} during amyloid formation by htt^{NT}-containing polyQ sequences. Mutations within htt^{NT} designed to diminish α-helical propensity diminish the aggregation of htt exon1 mutants[17] as well as some htt^{NT} targeting functions in the cell[16]. Independent of its initial conformation, it would be reasonable to expect that htt^{NT} might become incorporated into the β-stranded amyloid structure along with the polyQ elements. Thus, this is consistent with observations of transformations of native structure to amyloid β-structure (e.g. seen in the Josephin and

CRABP domains, as well as other proteins[32]). This expectation is also in line with simulations suggesting a conversion of α- to β-structure within htt^{NT} as a result of, or even a prerequisite for, amyloid formation[24]. Experimental data that seem consistent with a transition into β-structure include fluorescence data indicating that residues 11 and 17 within htt^{NT} in htt^{NT}-polyQ peptides become much more solvent-excluded as oligomers transition into amyloid fibrils [10].

Based on the use of magic-angle-spinning (MAS) solid-state (ss)NMR techniques[33] augmented by FTIR and electron microscopy (EM), we report here on the structure of fibrillar aggregates formed by the htt N-terminal fragment $htt^{NT}Q_{30}P_{10}K_2$ (Figure 1). Incorporation of ^{13}C,^{15}N-labels into residues within the N-terminal segment of this construct permitted site-specific characterization of residues within both the htt^{NT} and polyQ domains. This revealed a β-sheet structure for polyQ residues and for residues at the htt^{NT}-polyQ boundary, with spectroscopic signatures for the former that indicated a strong resemblance to glutamines in simple polyQ peptide fibrils. Surprisingly, our data also clearly indicated an α-helical segment in the N-terminal portion of the htt^{NT} sequence, which shows increased mobility and exposure to water compared to the rigid β-sheet core of the fibrils. FTIR suggests that a helical conformation is also likely the dominant secondary structural feature of the initially formed htt^{NT} oligomers. Thus, our data suggest that the htt^{NT} sequence exerts its dramatic ability to enhance the rate of formation of β-rich amyloid fibrils without either relinquishing its own initial α-helical structure or greatly influencing the β-sheet structure in the polyQ-rich core of the fibril.

Materials and Methods

Synthesis and fibril formation

Fmoc-protected ^{13}C- and/or ^{15}N-labeled amino acids were from Cambridge Isotope Laboratories (Andover, MA) and Isotec (Sigma-Aldrich, St. Louis, MO). Site-specifically labeled peptides were prepared by solid-phase peptide synthesis by the W.M. Keck Facility at Yale University (see also Table S2 in the Supporting Information). Crude peptide was purified in-house, disaggregated and fibrillized as described previously[10,34]. Briefly, fibril formation took place in PBS buffer at 37 °C and was monitored via HPLC-based sedimentation assays. The morphology of the mature fibrils was examined via TEM, using a FEI Tecnai 12 electron microscope (Hillsboro, OR), employing negative staining with 1% uranyl acetate.

Fourier transform infrared spectroscopy

Mature aggregated samples were studied by FTIR, using methods analogous to those described previously[10]. The FTIR samples were prepared by resuspension into 3μl of PBS of a pellet obtained by centrifugation at 20,817 × g for 45 min. The pelleted material was characterized using an MB series spectrophotometer (ABB Bomem, Quebec City, QC, Canada) and PROTA software from Biotools Inc, (Jupiter, FL). The FTIR data are reported as second-derivative spectra as calculated using the PROTA software.

Magic-angle-spinning solid-state NMR spectroscopy

After washing with 10mM sodium phosphate buffer, the mature fibrils were packed into MAS rotors (Bruker Biospin, Billerica, MA) by centrifugation, keeping them hydrated and unfrozen at all times. Unless indicated otherwise, NMR experiments were performed using a wide-bore Bruker Avance I spectrometer operating at 600 MHz ^1H Larmor frequency (14.3 T) using Bruker 3.2mm MAS EFree HCN probes. Some data were acquired on an Avance II spectrometer with a 800 MHz ^1H Larmor frequency (19 T). The sample temperature was controlled with cooled gas, but samples remained unfrozen. 2D ^{13}C-^{13}C experiments relied

on ^{1}H-^{13}C cross polarization (CP) followed by DARR mixing[35] for the ^{13}C-^{13}C transfers, with mixing times between 8 and 100ms, and 83–100 kHz ^{1}H TPPM decoupling[36] during acquisition and evolution. Additional ^{13}C SQ-DQ 2D experiments at 12kHz MAS and $\omega_{0,H}/2\pi$=600 MHz employed $SPC5_3$ to generate DQ coherence[37]. Inter-residue distance measurements in sample p4 ($htt^{NT}Q_{30}P_{10}K_2$ labeled with ^{13}C'-Leu7, $^{13}C\beta$-Ala10, ^{13}C'-Phe17) were performed at 600 MHz (^{1}H frequency) using a 4mm Bruker MAS HCN solenoid probe, employing PDSD ^{13}C-^{13}C recoupling. Water-filtered ^{1}H-^{13}C CP experiments that eliminate rigid ^{1}H signals via a T_2-relaxation filter and incorporate a ^{1}H-^{1}H spin diffusion period, were performed analogous to previously published methods (see also Figure S5 in the supporting information)[38,39]. Spectra were processed and analyzed with the aid of the NMRPipe, Sparky and CCPNMR/Analysis programs[40–42]. Indirect external referencing of the ^{13}C shifts relative to aqueous DSS was done based on the ^{13}C shifts of adamantane[43]. Secondary shift calculations involved subtraction of random coil shifts reported by Zhang et al[44]. Additional experimental details are listed in Table S3 in the SI.

Results

Aggregation kinetics and morphology

Consistent with previous results, the presence of the htt^{NT} segment in the $htt^{NT}Q_{30}P_{10}K_2$ construct strongly enhances its rate of aggregation compared to polyQ model peptides of an equivalent length (Figure 1). Transmission electron microscopy (TEM) shows that the morphology of the $htt^{NT}Q_{30}P_{10}K_2$ fibrils is similar to fibrils formed by analogous constructs with different polyQ lengths[10], but appears to differ from the polyQ peptide fibrils (Figure 2). The polyQ peptides form ribbon-like fibrils of variable width, whereas the fibrils formed by $htt^{NT}Q_{30}P_{10}K_2$ are more well-defined. As noted previously[10], the htt^{NT} segment itself is much less prone to aggregate, but does form a limited amount of an oligomeric aggregate, as shown in both Figure 1 and Figure 2. The morphology of these htt^{NT} aggregates resembles that of the characteristic oligomeric intermediates observed early in the aggregation of $htt^{NT}Q_{30}P_{10}K_2$ and other amyloid fibrils. As expected, the incorporation of ^{13}C and ^{15}N-labeled residues in various peptides does not noticeably affect the fibril morphology or aggregation kinetics (Figure 1; compare open symbols and grey circles), even without seeding with pre-existing aggregates.

Secondary structure analysis of aggregates by FTIR

The secondary structure content of the aggregated peptides was examined by FTIR spectroscopy. The results (Figure 2) show that the oligomeric aggregates formed by the isolated htt^{NT} peptide are predominantly α-helical in structure. Note that this is in contrast to the behavior of the monomeric peptide, which was previously found to be largely unstructured by solution NMR[10]. It is well known that simple polyQ model peptides aggregate into β-sheet rich fibrillar aggregates[26,47]. Amide I FTIR data on the $K_2Q_{31}K_2$ fibrils are consistent with this, showing strong bands characteristic of β-sheet[46] as well as bending and stretching modes associated with the glutamine side chain[48]. The FTIR spectrum of the $htt^{NT}Q_{30}P_{10}K_2$ fibrils is dominated by the same bands, as previously reported for related constructs[10]. Unfortunately, a complete overlap of the α-helix and glutamine side chain bands of the Amide I, as well as the limited ability of FTIR to give segment specific information, prevents us from extracting information on the secondary structure of htt^{NT} in these aggregates. Keeping in mind this ambiguity about the structure of the htt^{NT} segment in the fibrils and the limited resolution of the technique, our FTIR data are unable to show any structural difference between $htt^{NT}Q_{30}P_{10}K_2$ and $K_2Q_{31}K_2$ fibrils (even in the respective polyQ domains).

SSNMR chemical shift assignment

To obtain the required site-specific structural information we applied MAS ssNMR to study fibrils prepared from three differently labeled peptides, featuring U-^{13}C,^{15}N-labeled residues in selected positions (ref. Table S2 in the SI): Ala2, Leu7, Phe17 (sample p1); Ala10, Phe11, Leu14, Gln18 (sample p2); and Leu4, Lys6, Ser16, Gln19 (sample p3). 2D ^{13}C-^{13}C DARR experiments[35] were primarily used to assign the ^{13}C resonances (Table S1 in the S.I.). Representative 2D spectra with 25ms mixing time are shown in Figure 3. We observed single resonances for many of the labeled sites (Ala2, Leu4, Lys6, Leu7, Ala10, Phe11, Leu14). However, for several sites multiple signals were observed, most noticeably for the labeled glutamines at positions 18 and 19. The 2D DARR spectra show twice the cross-peaks expected for a single labeled glutamine, as highlighted in Figure 4a–b. Intriguingly, these doubled sets of resonances are nearly identical between Gln18 and Gln19. These observations indicate that both residues feature two distinct conformations with approximately equal intensity. In addition, within each conformer the chemical shifts of the glutamine Cβ and Cγ appear nearly identical. As these shift patterns are somewhat unusual, we obtained further evidence for this from 2D spectra that correlate single-quantum (SQ) and double-quantum (DQ) frequencies, employing SPC5$_3$ DQ mixing[37] (e.g. Figure 4d). Such spectra lack diagonal peaks (including the signals due to natural abundance ^{13}C sites), facilitating the identification of cross-peaks between nuclei with (nearly) identical shifts. Generally one expects pairs of peaks that bracket a pseudo-diagonal (shown in gray), reflecting directly bonded pairs of sites. If both carbons have identical frequencies, they show up as a single peak on this line, and we indeed observe this for the Gln19 Cβ and Cγ resonances of both forms. Analogous data were obtained for Gln18 (not shown). In addition to the doubling of the glutamine signals, we also observe doubling in Ser16 and Phe17, with the former being clearly visible in Figure 4d. Note that we currently lack the data to know how the two forms for these sequential “doubled” residues (marked ‘a’ and ‘b’ in the figures) correlate to each other.

Secondary structure identification

The observed chemical shifts were used to identify the secondary structure of the labeled residues via an approach that compares the shifts to those of the amino acids in defined secondary structures[49]. Figure 5 shows a graphical representation of the secondary shifts of the labeled residues, calculated through subtraction of random coil chemical shifts[44], along with a schematic showing how the secondary structure elements map onto the primary structure. Illustration of the consensus CSI and the Cα-Cβ chemical shift differences (which are insensitive to referencing differences) can be found in the SI (Figure S1). Residues 4, 6, 7, 10, and 11 are α-helical in structure. This is indicative of an amphipathic helix, as illustrated in Figure 5b. Residues 16–19 are predominantly in a β-sheet conformation, with one exception in that one of the two Ser16 forms is neither clearly β-sheet nor α-helical. Residues Ala2 and Leu14 also lack a defined secondary structure, thereby delimiting the length of the helical segment within the htt^{NT}domain. Our identification of the helix was further supported by the observation of an inter-residue (i → i+3) contact consistent with a helical rather than β-sheet conformation. A 2D ^{13}C-^{13}C proton-driven spin diffusion (PDSD) experiment on a sample (p4) specifically labeled in the ^{13}Cβ of Ala10 and ^{13}C’ of Leu7 yielded a cross-peak that is indicative of a distance of no more than 6Å, consistent with the presence of these two residues within an α-helix (Figure S2). We also tentatively identified the background ^{13}C signals due to the unlabeled prolines in the polyPro segment and found them to be similar to those reported for a PPII helical conformation[50] (see Figure S3).

PolyGlutamine structure and mobility

Given the striking similarity between the Gln18 and Gln19 conformations, we also probed the signals of a polyQ domain in fibrils of a polyQ peptide ($K_2Q_{30}K_2$) that was labeled in position Gln6 (i.e. the fourth glutamine). The NMR signals of this residue, which was chosen to avoid putative hairpin turns[51], showed doubling and chemical shifts that matched the data for Gln19 of $htt^{NT}Q_{30}P_{10}K_2$ fibrils (Figure 4). To investigate whether these site-specific data reflect the polyQ domains as a whole, we also examined fully unlabeled fibrils of a $K_2Q_{31}K_2$ and $htt^{NT}Q_{30}P_{10}K_2$ fibrils. In the absence of labeling, site-specific assignment is difficult, but the observed natural abundance ^{13}C signals in the 1D spectrum of $K_2Q_{31}K_2$ (Figure 6a) are expected to predominantly represent a summation of all its combined glutamine signals. Interpretation of the $htt^{NT}Q_{30}P_{10}K_2$ spectrum is not so straightforward, since it also includes numerous signals from the htt^{NT} and polyPro domains (Figure 6b). Fortunately, however, simple NMR experiments allow us to distinguish sites based on mobility differences. These measurements take advantage of the sensitivity of ssNMR experiments to local dynamics by comparing the observation of ^{13}C magnetization in direct polarization (DP) experiments with signals obtained by ^{1}H-^{13}C CP. In a DP experiment with short inter-scan times, the signal of rigid ^{13}C sites is attenuated due to their slow relaxation. In contrast, ^{1}H-^{13}C CP experiments disfavor mobile sites since the ^{1}H to ^{13}C transfer relies on the dipolar interaction, which is attenuated by dynamics. Indeed, in the $K_2Q_{31}K_2$ fibrils, most signals are eliminated in the DP spectrum indicating an overall rigidity of the polyQ amyloid fibrils. In contrast, many resonances in the $htt^{NT}Q_{30}P_{10}K_2$ fibrils show up strongly in the DP spectrum and are therefore much more mobile. Application of analogous experiments to the labeled peptides confirmed that these mobile sites are the non-β-sheet htt^{NT} residues, while the glutamine resonances are effectively 'filtered' out of the DP spectrum (see Figure S4).

Another way to highlight the most rigid sites is by simply subtracting the DP (mobile) signals from the CP spectrum. Applying this approach to the $htt^{NT}Q_{30}P_{10}K_2$ fibrils yields a very specific set of resonances that strongly resemble not only the $K_2Q_{31}K_2$ fibrils but also the peak positions and characteristic doubling of the labeled glutamine residues (Figure 6c). This indicates a strong resemblance between the molecular conformations of the polyQ domains in both the simple polyQ and $htt^{NT}Q_{30}P_{10}K_2$ contexts and suggests that the characteristic structural features shared by all of the labeled glutamines also extend to the bulk of the polyQ domain.

Water accessibility

As a picture arises in which the N-terminal helix is mobile and seemingly not incorporated into the amyloid fibril proper, we explored the water-exposure of different parts of these fibrils via relaxation-filtered MAS NMR. This is an approach previously applied to membrane proteins and amyloid fibrils[38,39,52]. Following a T_2 relaxation filter to select the highly mobile water protons, a ^{1}H-^{1}H diffusion period permits the monitoring of magnetization transfer back into the more rigid fibrils, observed as ^{13}C signals following ^{1}H-^{13}C CP transfer. The water-based origin of the ^{1}H polarization was confirmed using 2D ^{1}H-^{13}C spectra (not shown). The data on labeled samples p2 and p3 (Figure 7) reveal that residues in the htt^{NT} segment are polarized faster than either of the labeled glutamines. It also appears that the Gln19 sites are less accessible than Gln18. Even though a quantitative interpretation is not straightforward, since various polarization transfer mechanisms can be active in these experiments[53], it is clear that the N-terminal helix is more accessible to water than either of the labeled glutamine residues.

Discussion

N-terminal helicity

The first target in our investigation was the characterization of the conformation of the htt^{NT} segment in the mature amyloid fibrils. This short peptide element appears to initiate the aggregation mechanism of exon 1-like peptides, but only when attached to a polyQ sequence of significant length[10]. As a monomer in solution, the htt^{NT} segment by itself appears to exist as an ensemble of compact states that transiently sample α-helical conformations[10,16,25]. While enhanced helicity and self-association have been observed in certain contexts[10,54], whether and how the structure of htt^{NT} changes as the aggregation reaction initiates and proceeds has been unclear. The general ability of the amyloid motif to recruit peptide segments into β-structure suggests that the htt^{NT} segment might similarly be drawn into the β-structure amyloid core as the polyQ domain adopts it β-stranded amyloid conformation, and recently published molecular dynamics simulations[24] support this expectation.

Given the above context, our observations are of particular interest and somewhat surprising, since our ssNMR data on the fibrils clearly reveal helicity in residues spanning positions 4–11, which constitute an amphipathic helix (Figure 5b). Htt^{NT} as an amphipathic helix had previously been proposed as a functional unit, for instance as a membrane-binding targeting motif[16,20]. Amphipathicity and helicity have also been reported as essential for the htt^{NT}-dependent enhancement of fibrillization[16,17], and to affect toxicity and nuclear accumulation[16]. However, it has been difficult to obtain solid structural data to support the existence of this α-helix in a biologically relevant setting. In this work, we provide the first direct experimental data demonstrating the presence and precise location of the α-helical segment in the context of the amyloid-like fibrils. The observed helical segment is bracketed by non-helical residues, clearly showing that the α-helix does not span the whole htt^{NT}, contrasting with earlier X-ray data[54] and simulation results[31]. Instead, the observed α-helical segment appears to match well to experimental CD data suggesting 40–55% helical content[10,16,25] and certain simulations[17,31]. Solution NMR experiments indicate that in the isolated htt^{NT} the helicity may be transient, unstable and most pronounced in the N-terminal few residues[10].

Our FTIR data show that self-aggregation of the htt^{NT} peptide results in helical aggregates, suggesting that the helical structure is stabilized upon oligomerization. Through interacting with each other, the amphipathic htt^{NT} peptides may provide a much more hydrophobic environment than the monomer experiences in solution. This could significantly increase the stability of the helical conformation, in the oligomers and throughout the aggregation process. A recent X-ray study on a fusion construct consisting of a maltose-binding protein fused to the N-terminus of htt exon 1 (featuring 17 Gln residues in its polyQ domain) also revealed helicity in the htt^{NT} segment (and beyond).[54] Interestingly, the crystal contacts in these crystals included htt^{NT}-htt^{NT} interactions in a htt^{NT} helical bundle, possibly analogous to the types of interacting involved in the early aggregates. A picture arises in which isolated, monomeric htt^{NT} has a limited propensity to attain a partial helical structure, but that this propensity may be modulated by interactions involving membranes, the polyQ domain, other htt^{NT} molecules, or other proteins.

Glutamine amyloid core structure

As expected, the FTIR data show the presence of high β-sheet content in the $K_2Q_{31}K_2$ and $htt^{NT}Q_{30}P_{10}K_2$ fibrils. Based on NMR on the labeled $htt^{NT}Q_{30}P_{10}K_2$ fibrils, we also know that residues at the htt^{NT}-polyQ boundary (including Gln18 and Gln19) are in a β-sheet conformation. The observed rigidity and lack of water-exposure of the glutamines, which

extends into the side chains, is consistent with their being in a restricted and dehydrated polar-zipper or steric-zipper-like motif[55,56]. Among the β-sheet residues at the C-terminal end of the htt^{NT} domain, we do see that the Phe17 side chains experience substantial mobility (see Figure S3 in the SI). However, such dynamics do not necessarily require or imply solvent exposure of the Phe rings[57].

Both the FTIR and NMR data fail to show any obvious spectroscopic differences for the polyQ amyloid core of 'simple' polyQ fibrils compared to that of $htt^{NT}Q_{30}P_{10}K_2$ fibrils. More convincingly, we observed strikingly similar patterns of chemical shifts for both Gln18 and Gln19 in $htt^{NT}Q_{30}P_{10}K_2$ *and* for the Gln6 in $K_2Q_{30}K_2$. Our data also suggest that most of the glutamine residues within the rigid polyQ core feature the same two conformations that are present in these two site-specifically labeled glutamines. It is thought that the fibrillar polyQ should incorporate tight turns connecting extended β-strands[51], and it seems likely that the signals we observed reflect the residues that would occupy the β-strands.

One intriguing feature of all the β-sheet residues is that they present doubled sets of NMR resonances of roughly equivalent intensity. Multiplicity in amyloid fibril ssNMR signals is not uncommon and correlates to a heterogeneity of the molecular conformation within the sample. Polymorphism[23] of the macroscopic fibril structure is one potential source. There are several reasons that argue against fibril polymorphism in this particular case. First, no sign of polymorphism has been detected by EM or other methods. Second, we see no sign of doubling for the signals of any of the helical residues, indicating that any polymorphism would have to be restricted to the β-sheet residues without having any consequences for the helical residues. Furthermore, we observe essentially identical spectroscopic signatures (including resonance doubling) for Gln residues in aggregates of both simple polyQ and $htt^{NT}Q_{30}P_{10}K_2$ peptides; given the radically different kinetics and mechanisms by which these two types of polyQ-containing peptides aggregate[10,11], it is highly unlikely that both peptides would independently grow into identical mixtures of polymorphic structures. Similarly, the relative intensity of the doubled peaks appears relatively invariant between samples, whereas one may expect more variation if these reflected different polymorphic aggregates, each forming according to its own mechanism-based kinetics.

On the other hand, a 1:1 peak ratio would seem inherently consistent with homogeneous samples of certain supramolecular motifs. Since parallel, in-register β-sheet structures inherently feature a single conformation and thus a single NMR signal for each residue[56,58], it appears unlikely that the polyQ segment in the htt N-terminal fragment examined here exists in parallel, in-register β-sheets in the amyloid fibril. Other supramolecular assemblies are characterized by different numbers of resonances for each residue[59]. Thus, signal doubling might be due to a structural inequivalence of identical residues within the fibril assembly, as a consequence of anti-parallel and/or out-of-register arrangements. An anti-parallel assembly, as previously proposed based on X-ray diffraction studies of polyQ aggregates[26,27], could indeed generate two distinct conformations for each residue, thus explaining the doubled resonances. Another alternate (but not mutually exclusive) explanation could involve a systematic or 'random' register shift of different peptides within the amyloid core, combined with a basic structure where alternating (odd vs even numbered) residues feature distinct side chain conformations. Such a pattern may be accommodated by the uniform polyQ sequence and the resulting out-of-register assembly could be expected to feature distinct sets of shifts for each sequence position (despite being quite uniform in its overall assembly).

Implications for the aggregation mechanism

In summary, we have clearly demonstrated the precise location of a well-defined α-helix within the mature fibrils and found evidence suggesting the presence of α-helical structure in htt^{NT} oligomeric aggregates. In the fibrils, the N-terminal residues adopt a water-exposed and somewhat mobile helix packed against the highly rigid and dehydrated amyloid core formed by the glutamine residues. This polyQ amyloid core seems highly repetitive in its molecular structure and shows striking similarities to the simple polyQ fibrils.

These observations complement previous experimental results on the earlier stages of the fibril formation by analogous polypeptides, which revealed an accelerated pathway that includes the formation of at least one oligomeric intermediate initiated via htt^{NT} interactions. Our FTIR data indicate a high level of α-helicity to be formed upon self-aggregation of the htt^{NT} peptides. The amphipathic helix that we identified in the mature fibrils may thus also be present upon the initial assembly of oligomeric intermediates. While there had been indirect evidence of such an amphipathic helix being involved[17], structural data presented here explicitly reveal the existence of an α-helical htt^{NT} segment in both htt^{NT} oligomers and fibrils. These results argue against a model where the polyQ threshold length triggers fibril formation by permitting htt^{NT} to attain a β-conformation[24].

Helicity in the oligomeric intermediates involved in amyloid formation is actually not unprecedented and has even been suggested to play a direct role in their formation[60]. However, in such cases, including two papers published while this manuscript was in review, maturation of the fibrils leads to a conversion into β-sheet structure[60–64]. The coincidence of our data on htt^{NT}-polyQ peptides with recently published data on the islet amyloid polypeptide (IAPP) is, in fact, remarkable: monomeric IAPP lacks a stable helix in isolation, helicity is present in the oligomeric aggregates, which mature into β-stranded amyloid fibrils, and mutations designed to interfere with helix-helix interactions can abolish amyloid formation[63]. Highly similar considerations were also reported for very short designed peptides [64]. Our data provide a striking variation on this emerging theme, in which a helical element plays a critical role in the initial steps of amyloid formation, but *without* taking on β-sheet characteristics and *without* being incorporated into the amyloid core of the end stage fibrils.

An intriguing question is whether or how these observations affect the thinking about amyloid formation in a more general sense. For instance, the principles that have been applied in the design of computational models aimed at predicting amyloid formation rates from primary sequence information currently often reflect the compatibility of test sequences with a generic amyloid structural motif[65,66]. If there is indeed a critical role for helical conformations as well as non-local interactions (involving domains that never end up in an amyloid structure), then an over-reliance on compatibility with the *final* amyloid conformation may not fully capture the kinetics governing the formation process. In htt exon 1 aggregation it seems quite clear that the htt^{NT} segment provides an orders-of-magnitude boost in aggregation kinetics, as well as a dramatic change in mechanism (Thakur, 2009), while never itself engaging the cross-β amyloid motif. Naturally, it remains to be seen whether the mechanism by which htt^{NT} stimulates fibril formation is a rare oddity, or is a more common, but difficult to observe, phenomenon. Recent data on IAPP and other proteins (see above) lend some support to the latter point of view.

In terms of the mature amyloid core structure, the spectroscopic similarities between the polyQ domain within the htt N-terminal context and in the simple polyQ peptides indicate a resemblance in molecular structure. Given that amyloid structure can be very sensitive to the fibrillization conditions and mechanism, this would appear to imply that the polyQ β-sheet core in the htt-context might be formed along a similar pathway as occurs in the ‘simple’

polyQ systems. The role of the htt^{NT} may be mostly to bring the polyQ domains into close proximity, thus increasing the local concentration and permitting the fibril formation to start, without heavily modifying the resulting molecular structure. Note that the (local) polyQ concentration is known to have a large effect on the aggregation kinetics[4,6,11]. Thus, some of the structural and mechanistic lessons gleaned from studies of simple polyQ peptides may apply to features of htt fragments as well. This applies for instance to the observation that our NMR data show doubled chemical shifts specific to the β-sheet residues, raising doubts about assumptions of a parallel in-register conformation in the polyQ amyloid core[18,29]. Rather, it is perhaps more consistent with other arrangements like those proposed based on experimental data from simple polyQ fibrils[26,27]. As previously noted, unique supramolecular features may be facilitated by the uniform polyQ sequence, in contrast to amyloid fibrils with glutamine-rich, but more complex primary sequences[67].

These considerations then lead to a schematic picture of the aggregation process as illustrated in Figure 8. Key to this proposed pathway is the distinction between the roles of the N-terminal segment and the polyQ domain in the initiation of aggregation and the subsequent (but structurally separate) formation of amyloid structure and maturation into fibrils. Once an amyloid core has formed (i.e., is nucleated), it is likely that continued growth of the fibrils no longer relies on the htt^{NT}-htt^{NT} interaction. From the NMR data it is nonetheless clear that the htt^{NT} helical conformation is shared by all peptides throughout the fibrils. Various questions remain, such as the detailed molecular structure of the amyloid core and the nature of potential htt^{NT} interactions with itself, the polyQ domain or the polyPro PPII helix. Nonetheless, these new experimental data have clearly delineated key features of the process in vitro, which may well play similar roles in the aggregation process in vivo and thus affect the onset of the disease.

Supplementary Material

Refer to Web version on PubMed Central for supplementary material.

Acknowledgments

We thank Józef Lewandowski and Rakesh Mishra for helpful discussions and Mike Delk for technical support. This work was funded in part from startup funds from the University of Pittsburgh to PvdW, and by the US National Institutes of Health R01 grant AG 019322 to RW.

REFERENCES

1. Ross CA. Neuron. 2002; 35:819–822. [PubMed: 12372277]
2. Bates, GP.; Benn, C. Huntington's Disease. Bates, GP.; Harper, PS.; Jones, L., editors. Oxford, U.K.: Oxford University Press; 2002. p. 429-472.
3. Morley JF, Brignull HR, Weyers JJ, Morimoto RI. Proc. Natl. Acad. Sci. USA. 2002; 99:10417–10422. [PubMed: 12122205]
4. Scherzinger E, Sittler A, Schweiger K, Heiser V, Lurz R, Hasenbank R, Bates GP, Lehrach H, Wanker EE. Proc. Natl. Acad. Sci. USA. 1999; 96:4604–4609. [PubMed: 10200309]
5. Chen S, Berthelier V, Yang W, Wetzel R. J. Mol. Biol. 2001; 311:173–182. [PubMed: 11469866]
6. Chen S, Ferrone FA, Wetzel R. Proc. Natl. Acad. Sci. USA. 2002; 99:11884–11889. [PubMed: 12186976]
7. Bhattacharyya AM, Thakur AK, Wetzel R. Proc. Natl. Acad. Sci. USA. 2005; 102:15400–15405. [PubMed: 16230628]
8. Slepko N, Bhattacharyya AM, Jackson GR, Steffan JS, Marsh JL, Thompson LM, Wetzel R. Proc. Natl. Acad. Sci. USA. 2006; 103:14367–14372. [PubMed: 16980414]
9. Bhattacharyya A, Thakur AK, Chellgren VM, Thiagarajan G, Williams AD, Chellgren BW, Creamer TP, Wetzel R. J. Mol. Biol. 2006; 355:524–535. [PubMed: 16321399]

10. Thakur AK, Jayaraman M, Mishra R, Thakur M, Chellgren VM, Byeon I-JL, Anjum DH, Kodali R, Creamer TP, Conway JF, Gronenborn AM, Wetzel R. Nat. Struct. Mol. Biol. 2009; 16:380–389. [PubMed: 19270701]
11. Kar K, Jayaraman M, Sahoo B, Kodali R, Wetzel R. Nat. Struct. Mol. Biol. 2011 *in press*.
12. Ellisdon AM, Thomas B, Bottomley SP. J. Biol. Chem. 2006; 281:16888–16896. [PubMed: 16624810]
13. Robertson AL, Bottomley SP. Curr. Med. Chem. 2010; 17:3058–3068. [PubMed: 20629626]
14. Duennwald ML, Jagadish S, Muchowski PJ, Lindquist SL. Proc. Natl. Acad. Sci. USA. 2006; 103:11045–11050. [PubMed: 16832050]
15. Dehay B, Bertolotti A. J. Biol. Chem. 2006; 281:35608–35615. [PubMed: 16973603]
16. Atwal RS, Xia J, Pinchev D, Taylor J, Epand RM, Truant R. Hum. Mol. Genet. 2007; 16:2600–2615. [PubMed: 17704510]
17. Tam S, Spiess C, Auyeung W, Joachimiak L, Chen B, Poirier MA, Frydman J. Nat. Struct. Mol. Biol. 2009; 16:1279–1285. [PubMed: 19915590]
18. Liebman SW, Meredith SC. Nat. Chem. Biol. 2010; 6:7–8. [PubMed: 20016493]
19. Ratovitski T, Gucek M, Jiang H, Chighladze E, Waldron E, D'Ambola J, Hou Z, Liang Y, Poirier MA, Hirschhorn RR, Graham R, Hayden MR, Cole RN, Ross CA. J. Biol. Chem. 2009; 284:10855–10867. [PubMed: 19204007]
20. Rockabrand E, Slepko N, Pantalone A, Nukala VN, Kazantsev A, Marsh JL, Sullivan PG, Steffan JS, Sensi SL, Thompson LM. Hum. Mol. Genet. 2007; 16:61–77. [PubMed: 17135277]
21. Serio TR, Cashikar AG, Kowal AS, Sawicki GJ, Moslehi JJ, Serpell L, Arnsdorf MF, Lindquist SL. Science. 2000; 289:1317–1321. [PubMed: 10958771]
22. Chiti F, Dobson CM. Annu. Rev. Biochem. 2006; 75:333–366. [PubMed: 16756495]
23. Kodali R, Wetzel R. Curr. Opin. Struct. Biol. 2007; 17:48–57. [PubMed: 17251001]
24. Lakhani VV, Ding F, Dokholyan NV. PLoS Comput. Biol. 2010; 6:e1000772. [PubMed: 20442863]
25. Williamson TE, Vitalis A, Crick SL, Pappu RV. J. Mol. Biol. 2010; 396:1295–1309. [PubMed: 20026071]
26. Sharma D, Shinchuk LM, Inouye H, Wetzel R, Kirschner DA. Proteins. 2005; 61:398–411. [PubMed: 16114051]
27. Sikorski P, Atkins E. Biomacromolecules. 2005; 6:425–432. [PubMed: 15638548]
28. Darnell G, Orgel JPRO, Pahl R, Meredith SC. J. Mol. Biol. 2007; 374:688–704. [PubMed: 17945257]
29. Darnell GD, Derryberry J, Kurutz JW, Meredith SC. Biophys. J. 2009; 97:2295–2305. [PubMed: 19843462]
30. Ignatova Z, Thakur AK, Wetzel R, Gierasch LM. J. Biol. Chem. 2007; 282:36736–36743. [PubMed: 17942400]
31. Kelley NW, Huang X, Tam S, Spiess C, Frydman J, Pande VS. J. Mol. Biol. 2009; 388:919–927. [PubMed: 19361448]
32. Fändrich M, Fletcher MA, Dobson CM. Nature. 2001; 410:165–166. [PubMed: 11242064]
33. Tycko R. Q. Rev. Biophys. 2006; 39:1–55. [PubMed: 16772049]
34. O'Nuallain B, Thakur AK, Williams AD, Bhattacharyya AM, Chen S, Thiagarajan G, Wetzel R. Methods Enzymol. 2006; 413:34–74. [PubMed: 17046390]
35. Takegoshi K, Nakamura S, Terao T. Chem. Phys. Lett. 2001; 344:631–637.
36. Bennett AE, Rienstra CM, Auger M, Lakshmi KV, Griffin RG. J. Chem. Phys. 1995; 103:6951–6958.
37. Hohwy M, Rienstra CM, Griffin RG. J. Chem. Phys. 2002; 117:4973.
38. Kumashiro K, Schmidt-Rohr K, Murphy O, Ouellette K, Cramer W, Thompson LK. J. Am. Chem. Soc. 1998; 120:5043–5051.
39. Andronesi OC, von Bergen M, Biernat J, Seidel K, Griesinger C, Mandelkow E, Baldus M. J. Am. Chem. Soc. 2008; 130:5922–5928. [PubMed: 18386894]

40. Delaglio F, Grzesiek S, Vuister GW, Zhu G, Pfeifer J, Bax A. J. Biomol. NMR. 1995; 6:277–293. [PubMed: 8520220]
41. Vranken WF, Boucher W, Stevens TJ, Fogh RH, Pajon A, Llinas M, Ulrich EL, Markley JL, Ionides J, Laue ED. Proteins. 2005; 59:687–696. [PubMed: 15815974]
42. Goddard, TD.; Kneller, DG. SPARKY - NMR Assignment Program. 2006. *(http://www.cgl.ucsf.edu/home/sparky/)*
43. Harris RK, Becker ED, De Menezes SMC, Granger P, Hoffman RE, Zilm KW. Magn. Reson. Chem. 2008; 46:582–598. [PubMed: 18407566]
44. Zhang H, Neal S, Wishart DS. J. Biomol. NMR. 2003; 25:173–195. [PubMed: 12652131]
45. Jayaraman M, Kodali R, Wetzel R. Protein Eng. Des. Sel. 2009; 22:469–478. [PubMed: 19541676]
46. Jackson M, Mantsch HH. Crit. Rev. Biochem. Mol. Biol. 1995; 30:95–120. [PubMed: 7656562]
47. Chen S, Berthelier V, Hamilton JB, O'Nuallain B, Wetzel R. Biochemistry. 2002; 41:7391–7399. [PubMed: 12044172]
48. Venyaminov S, Kalnin NN. Biopolymers. 1990; 30:1243–1257. [PubMed: 2085660]
49. Wishart DS, Sykes BD. J. Biomol. NMR. 1994; 4:171–180. [PubMed: 8019132]
50. Kricheldorf H, Müller D. Int. J. Biol. Macromol. 1984; 6:145–151.
51. Thakur AK, Wetzel R. Proc. Natl. Acad. Sci. USA. 2002; 99:17014–17019. [PubMed: 12444250]
52. Huster D, Yao X, Hong M. J. Am. Chem. Soc. 2002; 124:874–883. [PubMed: 11817963]
53. Lesage A, Gardiennet C, Loquet A, Verel R, Pintacuda G, Emsley L, Meier BH, Böckmann A. Angew. Chem. Int. Ed. 2008; 47:5851–5854.
54. Kim MW, Chelliah Y, Kim SW, Otwinowski Z, Bezprozvanny I. Structure. 2009; 17:1205–1212. [PubMed: 19748341]
55. Perutz MF, Johnson T, Suzuki M, Finch JT. Proc. Natl. Acad. Sci. USA. 1994; 91:5355–5358. [PubMed: 8202492]
56. Nelson R, Sawaya MR, Balbirnie M, Madsen AØ, Riekel C, Grothe R, Eisenberg D. Nature. 2005; 435:773–778. [PubMed: 15944695]
57. Bajaj VS, Van der Wel PCA, Griffin RG. J. Am. Chem. Soc. 2009; 131:118–128. [PubMed: 19067520]
58. Van der Wel PCA, Lewandowski JR, Griffin RG. J. Am. Chem. Soc. 2007; 129:5117–5130. [PubMed: 17397156]
59. Nielsen JT, Bjerring M, Jeppesen MD, Pedersen RO, Pedersen JM, Hein KL, Vosegaard T, Skrydstrup T, Otzen DE, Nielsen NC. Angew. Chem. Int. Ed. 2009; 48:2118–2121.
60. Abedini A, Raleigh DP. Protein Eng. Des. Sel. 2009; 22:453–459. [PubMed: 19596696]
61. Narayanan S, Walter S, Reif B. ChemBioChem. 2006; 7:757–765. [PubMed: 16570324]
62. Anderson VL, Ramlall TF, Rospigliosi CC, Webb WW, Eliezer D. Proc. Natl. Acad. Sci. USA. 2010; 107:18850–18855. [PubMed: 20947801]
63. Liu G, Prabhakar A, Aucoin D, Simon M, Sparks S, Robbins KJ, Sheen A, Petty SA, Lazo ND. J. Am. Chem. Soc. 2010; 132:18223–18232. [PubMed: 21138275]
64. Hauser CAE, Deng R, Mishra A, Loo Y, Khoe U, Zhuang F, Cheong DW, Accardo A, Sullivan MB, Riekel C, Ying JY, Hauser UA. Proc. Natl. Acad. Sci. USA. 2011; 108:1361–1366. [PubMed: 21205900]
65. Maurer-Stroh S, Debulpaep M, Kuemmerer N, Lopez de la Paz M, Martins IC, Reumers J, Morris KL, Copland A, Serpell L, Serrano L, Schymkowitz JW, Rousseau F. Nat Methods. 2010; 7:237–242. [PubMed: 20154676]
66. Goldschmidt L, Teng PK, Riek R, Eisenberg D. Proc. Natl. Acad. Sci. USA. 2010; 107:3487–3492. [PubMed: 20133726]
67. Baxa U, Wickner RB, Steven AC, Anderson DE, Marekov LN, Yau W-M, Tycko R. Biochemistry. 2007; 46:13149–13162. [PubMed: 17953455]

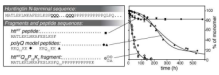

Figure 1.

Aggregation kinetics and peptide sequences. Aggregation kinetics were followed by a HPLC-based sedimentation assay, starting from disaggregated monomeric peptide. Labeled (open symbols) and unlabeled (grey circles, R^2 = 0.9912, SD= ±3.59) $htt^{NT}Q_{30}P_{10}K_2$ (at ~10 μM) show accelerated aggregation relative to peptide lacking htt^{NT}, e.g. 10 μM $K_2Q_{31}K_2$ (black triangles, R^2 = 0.9909, SD= ±4.02) or $K_2Q_{30}K_2$ (with [^{13}C,^{15}N-Gln6]; black diamonds, R^2 = 0.9926, SD= ±3.16). Note the qualitative difference in the initial rate regime. By itself, 10μM htt^{NT} (black squares, R^2 = 0.9534, SD= ±1.5169) shows only limited amount of aggregation.

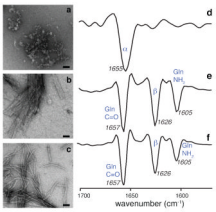

Figure 2.

Aggregate morphology and secondary structure. Negatively-stained transmission electron micrographs (left) and second-derivative FTIR data (right) of (a,d) htt^{NT} peptide aggregates, (b,e) mature fibrils formed by the polyQ model peptide $K_2Q_{31}K_2$, and (c,f) $htt^{NT}Q_{30}P_{10}K_2$. The TEM scale bars indicate a length of 50 nm. The htt^{NT} FTIR spectrum indicates substantial α-helical content, whereas that of the polyQ fibrils is dominated by the Gln signals and indicates β-sheet secondary structure[10]. Despite morphological differences by TEM, the $htt^{NT}Q_{30}P_{10}K_2$ FTIR data strongly resemble the polyQ results. No helical signals can be unequivocally identified due to the overlap between the Gln signals and the helical band. Band assignments: (d) 1655 cm^{-1}: α-helix; (e,f): 1657 cm^{-1}: Gln side chain C=O stretch; 1626 cm^{-1}: β-sheet structure; 1605 cm^{-1}: Gln side chain NH_2 deformation[45,46].

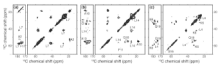

Figure 3.
2D ^{13}C-^{13}C ssNMR spectra using 25 ms DARR mixing, providing 1–2 bond transfers. Measurements on samples p1–p3 are shown in panels (a)–(c), with (a) obtained at 800MHz ^{1}H frequency and 16 kHz MAS, and (b, c) at 600 MHz ^{1}H frequency and 10 and 13 kHz MAS, respectively. Spinning side bands are marked with asterisks. For each spectrum aliphatic-to-carbonyl (left) as well as the intra-aliphatic (right) spectral regions are shown.

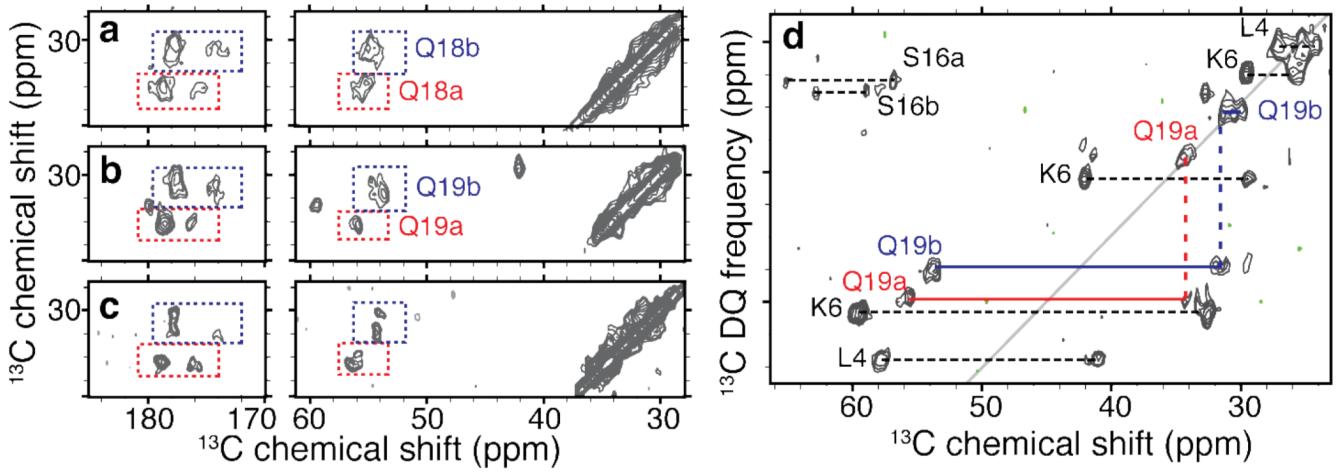

Figure 4.

Doubling and similarity of glutamine resonances. (a,b) 2D ^{13}C-^{13}C DARR spectral regions highlighting the Gln18 and Gln19 resonances in htt^{NT}Q$_{30}$P$_{10}$K$_2$ samples p2 and p3. For each residue we observe two distinct sets of resonances, marked as 'a' (red) and 'b' (blue). The cross-peak patterns suggest nearly identical chemical shifts for the Cβ and Cγ sites in each case. Panel (c) shows the virtually identical chemical shifts of a singly labeled glutamine within K$_2$Q$_{30}$K$_2$ fibrils (U-^{13}C,^{15}N-Gln6 - the fourth residue within the polyQ). (d) 2D ^{13}C-^{13}C SQ-DQ spectrum for sample p3 (using 1.5 ms SPC5$_3$ mixing at 12kHz MAS and $\omega_{0,H}/2\pi$=600 MHz), showing analogously color-coded Gln19 cross peaks. Doubling appears specific to the β-sheet structure: singular sets of resonances are observed for helical residues (e.g. Leu4), doubling can also be seen for Ser16.

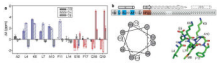

Figure 5.

Site-specific secondary structure assignment of $htt^{NT}Q_{30}P_{10}K_2$ fibrils. (a) Overview of secondary shifts (Δδ) of the labeled C', Cα and Cβ sites, revealing helicity (blue) in residues spanning the residues 4–11, whereas β-sheet structure (red) is seen in residues 16–19. Residues 2 and 14 match neither β-sheet nor a-helical conformations (black). Asterisks mark unobserved labeled sites. Bars are split for sites where two conformations were detected (based on doubled chemical shifts). (b) Schematic representation of observed secondary structure alongside the primary sequence (top), with the labeled residues in bold and color-coded as in (a). Bottom: helical wheel view of the helical segment (observed helicity spans the residues in grey) and a schematic illustration of the amphipathic helix, showing the distribution of hydrophobic residues (front and down) and charged residues (upward) with arbitrary side-chain conformations (prepared using PyMOL, Schrödinger, LLC). The blue dashed line indicates the observed inter-residue contact between Ala10-Cβ and Leu7-CO (Figure S2).

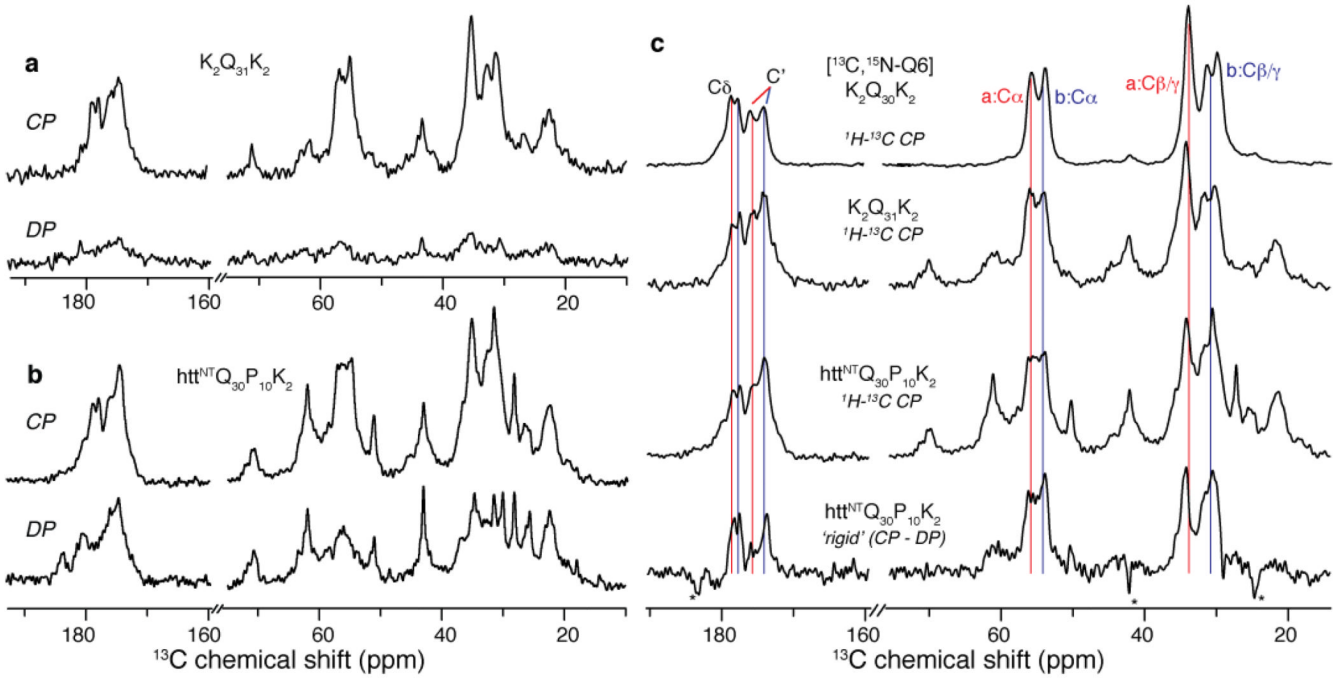

Figure 6.

PolyQ amyloid core and the effect of the htt^{NT} domain. (a) ^{1}H-^{13}C CP (top) and direct ^{13}C polarization (DP; bottom) of unlabeled $K_2Q_{31}K_2$ fibrils. These rigid sites are largely absent from the DP spectrum due to the short recycle delay (3 s). (b) Analogous spectra for unlabeled $htt^{NT}Q_{30}P_{10}K_2$ fibrils indicating increased mobility in many sites. (c) Subtraction of mobile sites in the DP spectrum for $htt^{NT}Q_{30}P_{10}K_2$ from its CP spectrum (3rd row) reveals the most rigid sites in this sample (bottom). These sites match the pattern of rigid polyQ signals in unlabeled $K_2Q_{31}K_2$ fibrils (2nd row), as well as the signal from the singly labeled Gln6 in $K_2Q_{30}K_2$ (top), which is virtually identical to Gln19 in the $htt^{NT}Q_{30}P_{10}K_2$ fibril core (Figure 4). Thus, the site-specifically labeled glutamine resonances are seemingly unaffected by the presence of htt^{NT}, and appear to be representative of the bulk of the glutamines in both $htt^{NT}Q_{30}P_{10}K_2$ and simple polyQ fibrils.

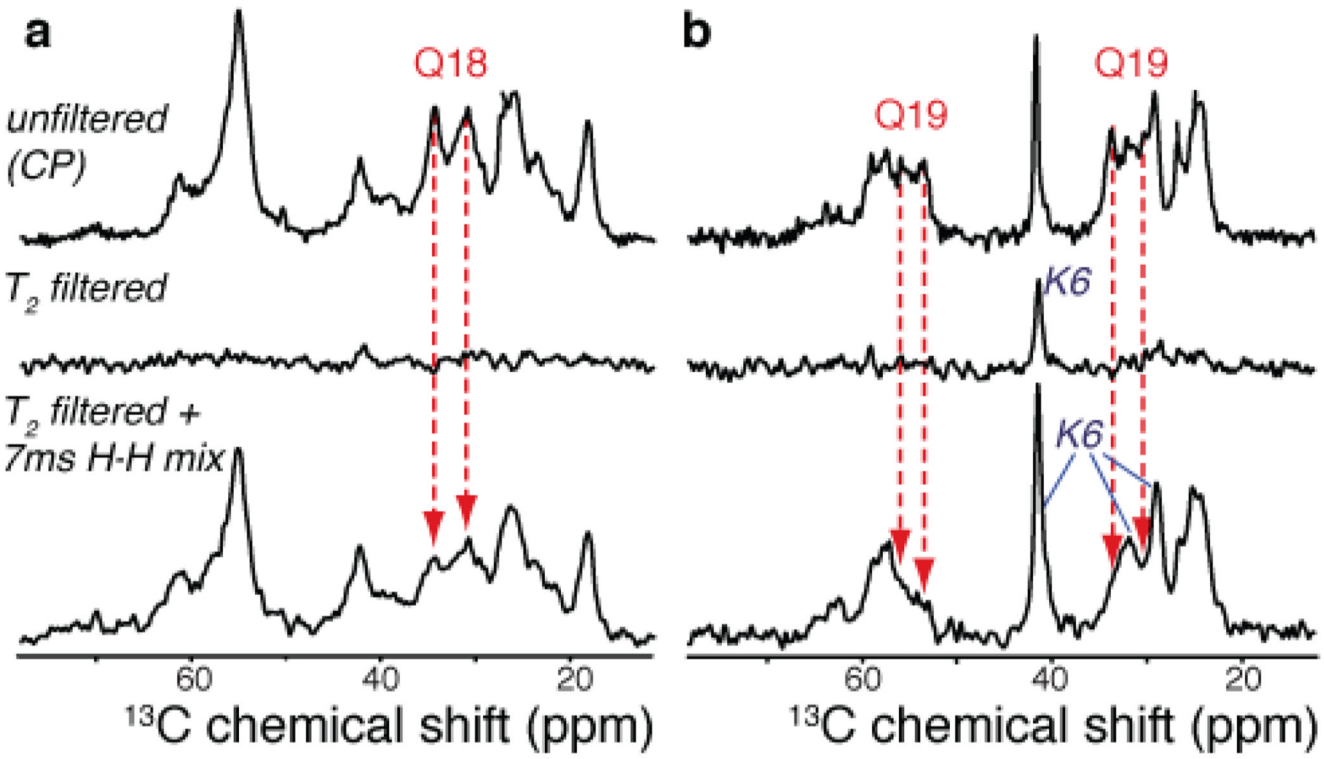

Figure 7.

^{13}C-detected water-filtered CP experiments on samples p2 (a) and p3 (b). The top row shows the ^{1}H-^{13}C CP signals in the absence of a T_2 filter. A water-proton-selective T_2 filter eliminates virtually all peptide signals (middle row). 7ms ^{1}H-^{1}H longitudinal mixing results in ^{1}H polarization transfer from water into the fibrils (bottom). Gln18 and especially Gln19 signals remain suppressed in the water-filtered spectra (red arrows), whereas sites in the htt^{NT} helix are easily polarized (e.g., Lys6 in sample p3).

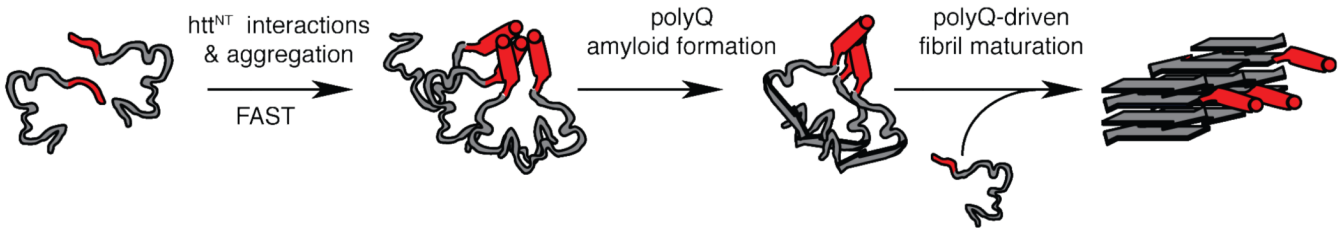

Figure 8.

Schematic model of htt^{NT}-initiated aggregation process. (a) In solution, the monomeric species lacks a well-defined structure. The htt^{NT} segment may have some helical propensity, but appears to lack a stable α-helical structure. (b) The htt^{NT} segment initiates the aggregation process, mediated by htt^{NT}-htt^{NT} interactions resulting in oligomeric species featuring substantial helicity. (c) This leads to a much-increased local polyQ concentration and permits the formation of the amyloid core, involving the generation of β-sheet secondary structure within the polyQ stretch. (d) Upon maturation, a highly rigid and dehydrated amyloid core (consisting of the polyQ) is decorated with the N-terminal residues 4–11 persisting in an α-helix that is relatively mobile and solvent exposed. Not shown is the polyPro domain that forms an immobilized PPII helix in the mature fibrils.